Int J Fract
DOI 10.1007/s10704-007-9134-x

ORIGINAL PAPER

J-integral evaluation for U- and V-blunt notches under Mode I loading and materials obeying a power hardening law

F. Berto · P. Lazzarin · Yu. G. Matvienko

Received: 3 April 2007 / Accepted: 2 October 2007

Abstract The paper deals with calculations of the J-integral for a plate weakened by U- and V-blunt notches under mode I loading in the case of a linear and nonlinear elastic material. The main aim of the study is to suggest simple equations suitable for rapid calculations of the J-integral. The semicircular arc of the notch, which is traction free, is assumed as integration path and the J-integral is given as a function of the strain energy over the notch edge. For a numerical investigation of the strain energy density distribution on the notch edge the equation $W(\theta) = W_{\max} \cos^{\delta}(\theta)$ has been assumed, where δ has been determined from finite element analyses. In particular, the following values of the notch acuity a/ρ and the opening angle 2α have been analyzed: $4 \le a/\rho \le 400$ and $0 \le 2\alpha \le 3\pi/4$. Considering plates weakened by lateral and central notches under symmetric mode I loading, the approximate relationships for the strain energy density, which require the presence of a non zero notch radius for their application, and the J-integral are discussed firstly considering a linear elastic material and then a material obeying a power hardening law during the loading phase. The predicted results of the J-integral are consistent with those directly obtained from finite element analyses.

Keywords Strain energy density distribution · J-integral · U- and V-notches · Finite element results

F. Berto · P. Lazzarin
Department of Management and Engineering, University of Padova, Stradella S. Nicola 3, 36100 Vicenza, Italy

Yu. G. Matvienko (✉)
Mechanical Engineering Research Institute, Russian Academy of Sciences, 4 M. Kharitonievsky Per., 101990 Moscow, Russia
e-mail: matvienko7@yahoo.com

Nomenclature

a	Notch depth (lateral notch) or notch semi-depth (central notch)
B	Width of the specimen
E	Young's modulus
J	J-integral (as due to the notch arc)
J_e	J-integral under linear elastic conditions
K	Constant in the Ramberg-Osgood law
$K_{t,g}$	Theoretical stress concentration factor
n	Hardening exponent in the Ramberg-Osgood law ($1 \le n < \infty$)
r	Distance from the notch tip
W	Strain energy density on the semicircular edge of the notch
2α	V-notch opening angle ($2\alpha = 0$ in a U-notch)
δ	Exponent in the equation of the strain energy density
ν	Poisson's ratio
θ	Angular coordinate
ρ	Notch radius
σ_0	Yield stress (0.2% offset stress)
σ_g	Remotely applied tensile stress
$\sigma^B_{\max}$	Beltrami equivalent stress at the notch tip

1 Introduction

The J-integral is a commonly used nonlinear fracture parameter for the description of the local fields in the neighbourhood of stress concentrations and for the analysis of crack initiation and propagation. The J-integral was thought of as the generalisation of the strain energy release rate to cases of nonlinear-elastic stress-strain curves (Rice 1968). However, for most cases of engineering interest, the nonlinear stress-strain behaviour is due to elastic–plastic behaviour, as in metals. For elastic–plastic materials J loses its interpretation in terms of potential energy available for crack extension, but retains physical significance as a measure of the characteristic crack-tip stress and strain fields around the crack tip (Dowling 1993).

Numerical methods allow us to evaluate the J-integral for any body configuration with a crack as well as type of loading (Atluri 1986, Anderson 2005). However, the numerical analysis is expensive and time-consuming to be used routinely in engineering calculations. Another problem is the difficulty to transfer the numerical results from one geometry to another, considering also the differences in the properties of the materials. At the same time, only a limited number of analytical solutions are presented in the literature (Shih and Hutchinson 1976; Kumar et al. 1981, 1984; Kumar and German 1988; Zahoor 1989; Saxena 1998; Matvienko and Morozov 2004; Anderson 2005) and these solutions mainly refer to cracked specimens made of materials obeying a power hardening law.

In the case of a sharp V-notch under linear elastic conditions, the local stress components follow Williams' exact solution (Williams 1952) and the stress intensity in the vicinity of the zone of singularity is generally quantified by means of the Notch Stress Intensity Factors (NSIFs) (Gross and Mendelson 1972). In contrast with the crack case, there is no possibility to correlate the J-integral to the NSIF of sharp V-notches, mainly because the J-integral is dependent on the arbitrary selected close contour connecting two points of the V-notch surfaces. However, as soon as the radius r of a semicircular path, at power $2\lambda_1 - 1$, is used to normalize J (the path being fully included in the zone governed by the Mode I singularity, $1 - \lambda_1$), the parameter $J_L = J/r^{2\lambda_1 - 1}$ returns to being path-independent (Lazzarin et al. 2002). It is clear that, contrary to the crack case, the straight flanks of the notch (and not only the V-notch tip) contribute to J and J_L.

Recently, the J-integral's properties were investigated for blunt U- and V-notches by means of analytical and numerical analyses (Livieri 2003; Chen and Lu 2004). In particular, Livieri (2003) demonstrated that if an appropriate integration path is chosen, there always exists an operator $J_{L\rho}$ that is invariant with respect to a particular semicircular path and coincides with $J_L = J/r^{2\lambda_1 - 1}$ pertaining to a sharp V-notch of the same depth. The operator $J_{L\rho}$ was later correlated to the relevant NSIF both of the blunt notch and of the sharp notch, making it possible to evaluate the theoretical stress concentration factor K_t for a blunt V-notch. The contribution to J provided by the notch flanks and the semicircular arc describing the notch root was discussed in detail also by Chen and Lu (2004). By using the J_i vector, it was confirmed that the J-integral for a blunt V-notch is always path-dependent, whereas for a U-notch the path independence of the J-integral requires certain conditions, namely, that the integration path completely encloses the notch root even if the remote loading is symmetric. Chen and Lu (2004) noted that the contribution to the J-integral induced by the arc describing the notch root might explain why there is a large scatter in the fracture toughness and fatigue data measured by means of the compliance technique by different researchers for nominally identical materials.

Neuber (1958, 1985) formulated the idea that in the presence of a sharp notch the material is sensitive to a fictitious root radius that depends on the material's 'micro structural support-length', linked to the concept of 'elementary volume'. This concept was reconsidered in some recent papers where the strain energy density was evaluated over a given finite size volume surrounding the tip of sharp and blunt V-notches subjected to Mode I loading. By using the mean value of the strain energy density (SED), the static strength properties of brittle engineering components weakened by sharp V-notches (Lazzarin and Zambardi 2001; Yosibash et al. 2004) and blunt V-notches under Mode I or mixed (Mode I and Mode II) loading (Lazzarin and Berto 2005a, b; Gómez et al. 2007), were treated in a unified manner, as was done for the high cycle fatigue strength properties of welded joints made of steels or aluminium alloys (Lazzarin and Zambardi 2001; Lazzarin et al. 2003; Livieri and Lazzarin 2005). In the case of brittle failures under static loads, the SED method was validated by using a large body of experimental data taken from the literature, mainly due to Carpinteri

(1987), Seweryn (1994), Seweryn et al. (1997), Dunn et al. (1997a, b), Gómez and Elices (2003, 2004), Gómez et al. (2005, 2007).

With the progress in computing, it is now possible to evaluate the actual stress distribution in the vicinity of a notch, independently of the complexity of the geometry. In the last years, an approach based on a volume definition was developed in Notch Fracture Mechanics also by Pluvinage (2003).

In parallel, a bridging between the elastic strain energy $E^{(e)}$ and the J-integral has been established considering a given critical volume. Such a volume is simply a circular sector of radius R_c in the case of sharp V-notches, and becomes a semi-moon embracing the notch edge in the case of blunt notches, leaving unchanged the material parameter R_c on the notch bisector line (see Fig. 1; Lazzarin and Berto 2005a, b). R_c works like Neuber's 'microstructural support length'. Close form expressions linking $E^{(e)}$, J-integral, the structural volume and the notch stress intensity factors were given for U- and V-notches under mode I loading (Berto and Lazzarin 2007).

Analytical calculation of the J-integral for a body with a U-notch was performed by Matvienko and Morozov (2004) considering a linear elastic and nonlinear elastic behaviour of the material. The integration path was chosen as the complete semicircular contour of the notch. In this case, the new equations based on stress concentration analysis and on the method of sections were proposed. The formulas were employed for bodies weakened by cracks and U-notches. Furthermore, the approach was also applied to the case of cracks emanating from the notches and to the critical state of short notches. As a result, these approximate solutions allow us to calculate the maximum stress and strain intensity on the surface of the notch tip using the notch radius, some mechanical properties of the material (the yield stress and the hardening exponent) and the J-integral. The tendency of the J/J_e ratio (J_e being the J-integral for an ideally linear elastic material) was found to be analogous to that of a notched body with a short crack at the notch tip, the crack length being less than the radius of curvature of the notch. Due to their nature, the equations proposed by Matvienko and Morozov (2004) work well when the notch acuity (notch depth a to notch radius ρ) tends to infinity.

The aim of the present paper is to analyze the effect of the notch acuity on the J-integral expressions and to give a set of useful formulas for plates weakened by U- and V-blunt notches under mode I loading in the case of a linear and nonlinear elastic material. The approximate equations, which take advantage of accurate results from finite element analyses, permit the rapid evaluation of the contribution to J-integral due to the circumferential arc describing the notch root. In the case of V-notches, where the J-integral is path-dependent, the contribution of the straight edges is not included. This means that the relevant, material-dependent, semi-moon-like volume shown in Fig. 1 should embrace entirely (or partially) the notch root but not the straight edges of the notches and this is a limitation of the paper. However, some numerical plots including the sharp, zero radius, V-notches will permit to understand the different contributions due to the notch arc and the notch flanks and to create a link between the J-integral approach and the approach based on the strain energy over a control volume, where the control radius is thought of as a material property.

2 Materials and geometry of the notched plates

In the present paper, a body with a U- and V- blunt notch under a remotely applied tensile stress σ_g has

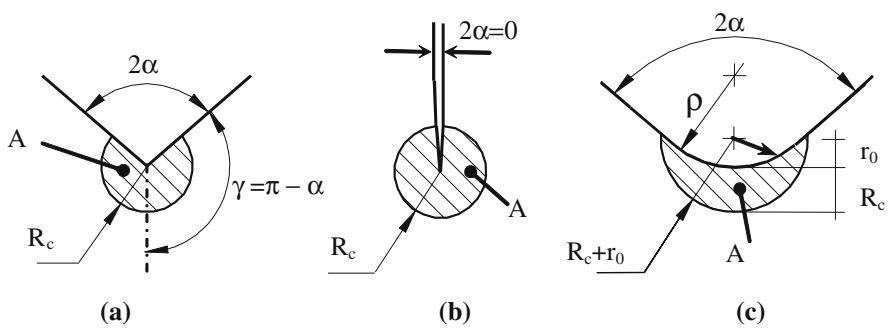

Fig. 1 Control volume (area) for sharp V-notch (**a**), crack (**b**) and blunt V-notch (**c**) under Mode I loading

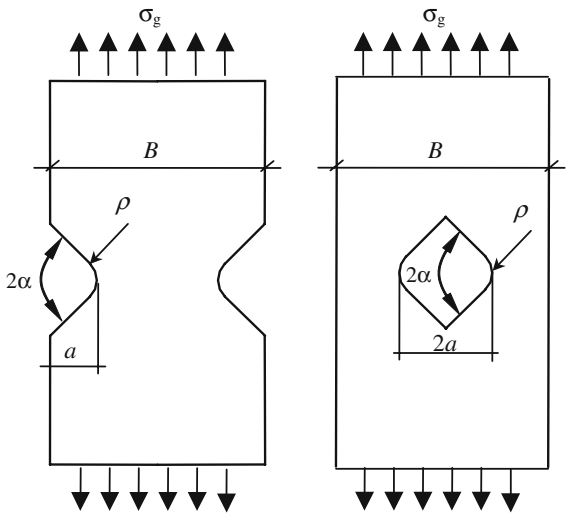

Fig. 2 Geometry of the specimens

been considered (Fig. 2). A multi-parametric analysis has been carried out considering a large variability of the ratio $a/\rho (4 \leq a/\rho \leq 400)$ and of the notch opening angle $2\alpha (0 \leq 2\alpha \leq 135°)$. In order to analyze the effect of different load intensities on the strain energy density and J-integral formulations, different stress levels were applied to the plates. All results are related to the loading phase, when stress increases monotonically, excluding the unloading phase as well as cyclic loading cases.

In the FE analysis the ratio of the width B to the notch length a has been kept constant and equal to 5. However, the set of equations presented in the present paper can be used for all cases with $B/a \geq 5$. In order to evaluate the effect of different strain hardening behaviours, two different common steels have been analyzed. These materials follow the Ramberg-Osgood law $\varepsilon = \sigma/E + (\sigma/K)^n$ and their properties are the following:

$$\text{AISI 1008,}\ \ K = 600\,\text{MPa},\ n = 4,\ \sigma_0 = 125\,\text{MPa},\quad E = 206\,\text{GPa},\ \nu = 0.3.$$

$$\text{AISI 1045,}\ \ K = 950\,\text{MPa},\ n = 8.33,\ \sigma_0 = 450\,\text{MPa},\quad E = 206\,\text{GPa},\ \nu = 0.3.$$

Here, E is Young's modulus, K is the material constant, n is the hardening exponent, ν is Poisson's ratio and, finally, σ_0 is the yield stress.

3 The strain energy density for central and lateral U-notches under linear elastic conditions

A notch of length a with the curvature radius ρ at the notch tip has parallel flat surfaces. The J-integral is represented as a contour integral according to Rice (1968) and Cherepanov (1979). At the same time, the J contour integral is equal to the energy release rate for a linear or nonlinear elastic material under quasi-static conditions (Anderson 2005). Thus, the J-integral can be viewed as both a contour integral and an energy parameter.

If integration path is the arc of the notch tip, which is traction-free, the J-integral can be evaluated by means of the expression:

$$J = \int_{-\pi/2}^{\pi/2} W(\theta)\rho\cos(\theta)d\theta, \tag{1}$$

where $W(\theta)$ is the strain energy density, ρ is the radius of curvature and θ is the angular coordinate of points on the notch edge. The polar coordinate system has its origin located at the notch center. Equation 1 was used by Matvienko (1994) to develop some expressions useful to evaluate J for a power hardening material. As a first approximation, the distribution of the strain energy density on the surface of the notch arc was assumed in the form (Matvienko 1994; Matvienko and Morozov 2004)

$$W(\theta) = W_{\max}\cos(\theta), \tag{2}$$

$W_{\max}$ being the maximum strain energy density at the notch tip. Strictly speaking, Eq. 2 is valid only in the case of $a/\rho \rightarrow \infty$. A more general law for $W(\theta)$, which should be valid also in the case of finite values of the notch acuity a/ρ, is assumed here according to the following relationship:

$$W(\theta) = W_{\max}\cos^{\delta}(\theta), \tag{3}$$

where δ is the exponent to evaluate by means of FE analysis. It is necessary to notice that Eq. 3 is an empirical guess based on a best fit of numerical results from mode I loading, the starting point, however, being Eq. 2 valid for an infinite plate weakened by U-notches with a strong acuity.

Some plots of the strain energy density on the notch edge for different values of a/ρ are shown in Figs. 3

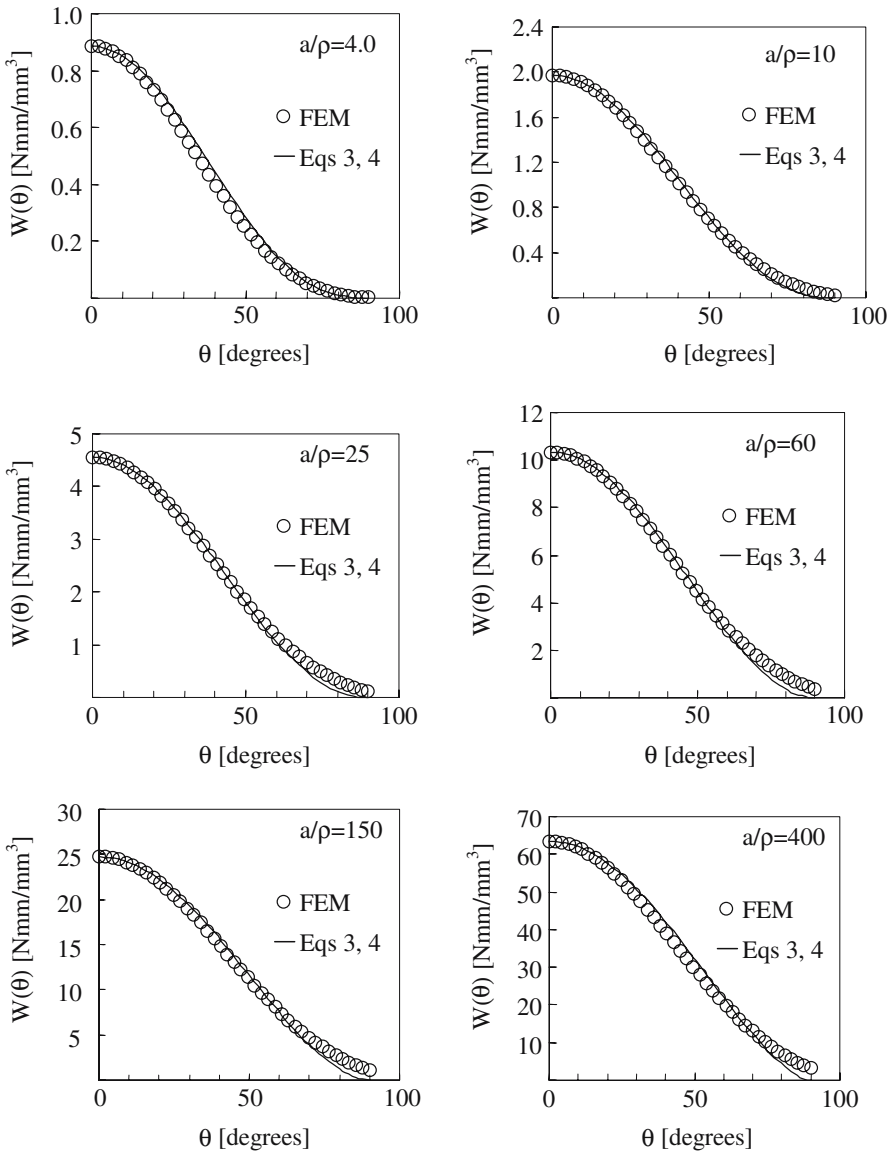

Fig. 3 Strain energy density along the notch for lateral U-notches having different acuity a/ρ. The applied nominal stress σ_g was equal to 100 MPa

and 4. Under a linear elastic hypothesis and plane strain conditions, the exponent δ depends only on the U-notch acuity. The relevant values for δ are listed in Table 1, as obtained by means of a best-fit analysis on the FE data. In particular, two different expressions have been obtained by interpolation of the numerical results from lateral and central notches under mode I loading. The expressions for the exponent δ is a function of a/ρ are:

$$\delta = 3.005 \left(\frac{a}{\rho}\right)^{-0.112} \quad \text{for} \quad 4 \le a/\rho \le 400 \qquad (4)$$

for lateral U-notches, and

$$\delta = 4.764 \left(\frac{a}{\rho}\right)^{-0.180} \quad \text{for} \quad 4 \le a/\rho \le 400 \qquad (5)$$

for a central U-notch.

The maximum difference between the values of Table 1 and those provided by Eqs. 4 and 5 is less than 1 percent. It should be noted that, at the same value of the notch acuity, the exponent δ is higher for central notches than for lateral notches. The difference decreases as the ratio a/ρ increases.

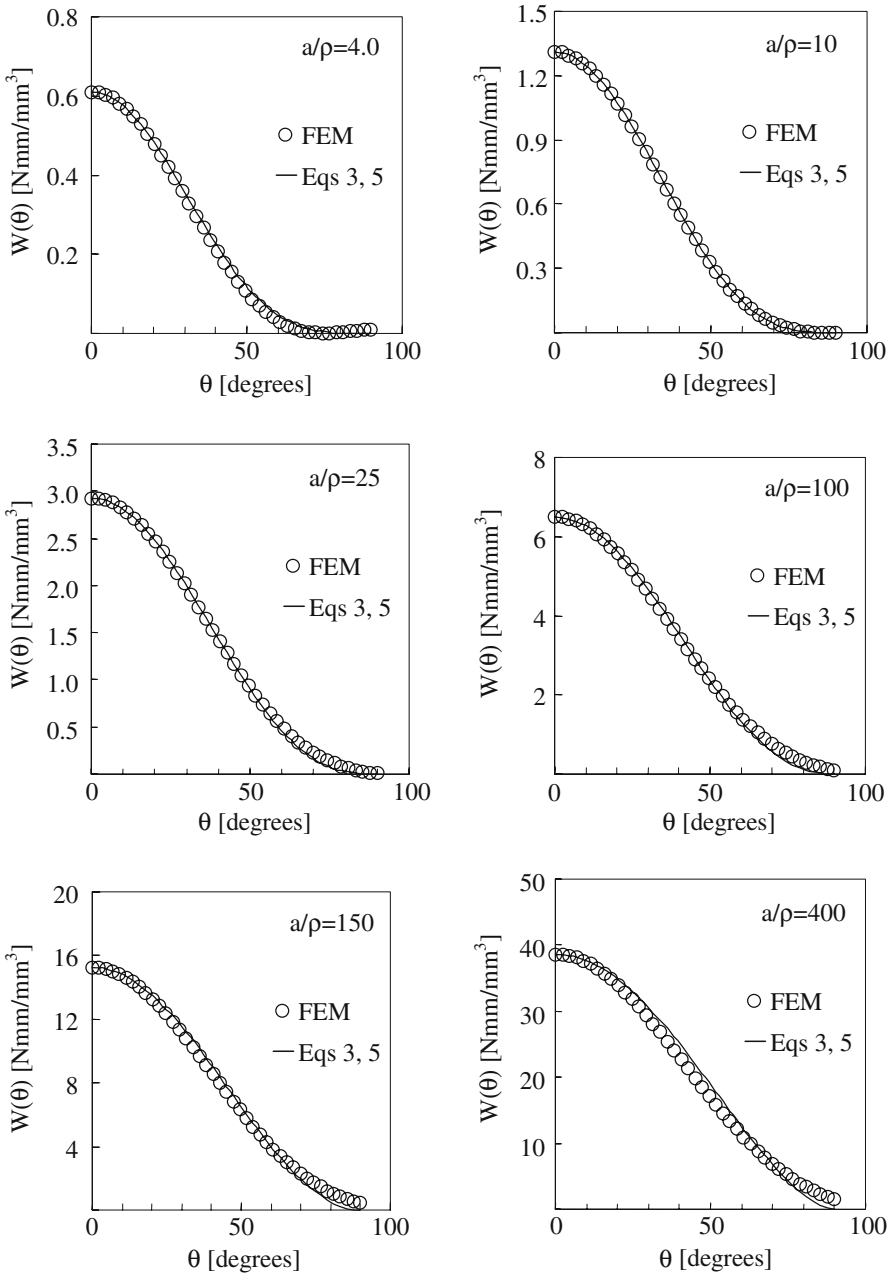

Fig. 4 Strain energy density along the notch edge for central U-notches having different acuity a/ρ. The applied stress σ_g was equal to 100 MPa

Recently, while considering U-notches under mixed mode loading, Gómez et al. (2005) extended the strain energy density approach by rigidly rotating a given control volume, as previously defined under mode I loading (Fig. 5a). All specimens were made of PMMA and tested at −60°C, a temperature able to assure a linear elastic behaviour. This volume was simply centred with respect to point P on the notch edge where the principal stress reached its maximum value (Fig. 5b). The 'effective' Mode I loading was justified by the strain energy density distribution, which resulted substantially symmetric with respect to the line crossing the point and normal to the notch edge (Gómez et al. 2007). This means that Eq. 3 can be applied also to mixed mode conditions moving the origin of the reference system from the notch bisector to the point of maximum principal stress, at least when the arc $A\hat{P}C$ is small with respect to entire semicircular root. When

Table 1 The value of δ for lateral and central U-notches as a function of the notch acuity under linear (L) or nonlinear (NL) elastic conditions

	Notch acuity a/ρ	L-elastic δ	NL-elastic δ
Central U-notches	4	3.71	3.93
	10	3.15	3.17
	25	2.67	2.57
	60	2.28	2.09
	150	1.93	1.69
	400	1.62	1.35
Lateral U-notches	4	2.57	2.68
	10	2.32	2.22
	25	2.10	1.83
	60	1.90	1.52
	150	1.71	1.26
	400	1.54	1.02

this condition is not satisfied, more precise calculations of the J-integral under mixed loading can be performed by using the inner arc $\widehat{ABC}$ and involving J_1 and J_2 components of J-integral (Gdoutos et al. 2003; Chen and Lu 2004).

Some results are shown in Fig. 5 with reference to both experimental data and theoretical predictions from U-notched specimens under mode I loading (Fig. 5a) and some results from mixed mode loading (Fig. 5b). With a control radius $R_c = 0.035$ mm (as determined on the basis of the ultimate tensile stress σ_u and the fracture toughness K_{IC} of the material), predictions of the critical loads to static failure based on the critical values of the strain energy density W_c match those based on the J-integral to arc $\widehat{ABC}$ ratio in all the cases considered here and are in a good agreement with the experimental data.

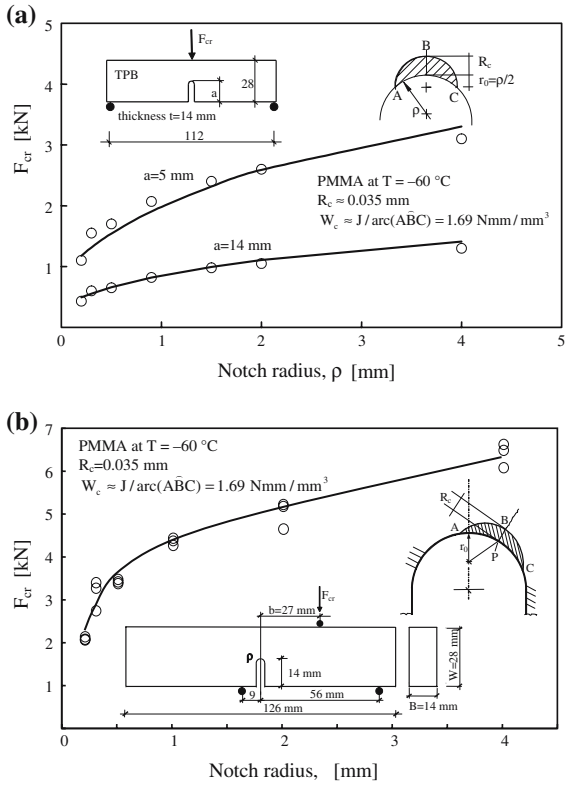

Fig. 5 Critical load F_{cr} versus notch radius ρ; comparison between theoretical predictions and experimental data for specimens made of PMMA tested at −60°C (experimental data from Gómez and Elices 2004, Gómez et al. 2007); (**a**) Mode I loading; (**b**) Mixed mode loading. Elastic modulus $E = 5050$ MPa, Poisson's ratio $\nu = 0.4$, ultimate tensile strength $\sigma_u = 130$ MPa, fracture toughness $K_{IC} = 1.8$ MPa m$^{0.5}$. Predictions based on constant values of $W_c = \sigma_u^2/2E = 1.69$ MJ/m^3 and $R_c = 0.035$ mm

4 Strain energy density for blunt V-shaped notches under linear elastic conditions

When the opening angle 2α is different from zero, the exponent δ in Eq. 3 depends both on the angle 2α and on the ratio a/ρ. In the FE analysis, the following values have been considered:

$$a/\rho = 4;\ 10;\ 25;\ 60;\ 150;\ 400 \quad \text{and}$$
$$2\alpha = 60°,\ 90,\ 135°.$$

As a result, different expressions are given for lateral and central notches under mode I loading. Namely, for lateral V-notches the equation is:

$$\delta\left(\frac{a}{\rho}, 2\alpha\right) = 3.005\left(\frac{a}{\rho}\right)^{-0.112} + 0.335\,(2\alpha)^{3.10}$$
$$\text{for} \quad 4 \le a/\rho \le 400 \quad \text{and} \quad 0 \le 2\alpha \le 3\pi/4 \qquad (6)$$

where the angle 2α is in radians. It should be noted that the first term on the right hand side of Eq. 6 matches Eq. 4 already proposed for lateral U-notches. The distribution of the strain energy density $W(\theta)$ on the edge for two symmetric V-notches is shown in Fig. 6 together with a comparison with Eq. 6.

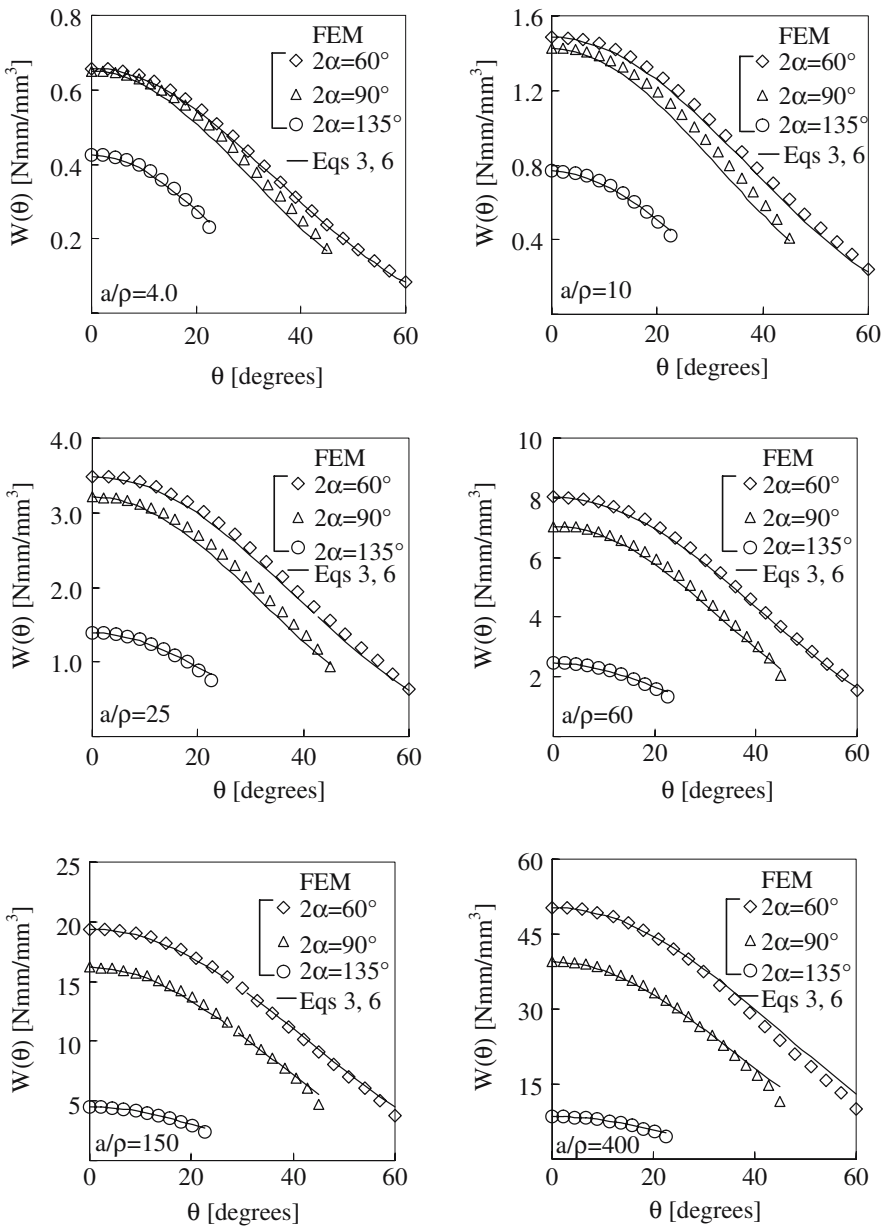

Fig. 6 Strain energy density along the notch edge for lateral V-notches having different acuity a/ρ. The applied nominal stress σ_g was equal to 100 MPa

For central V-notches two equations are proposed, depending on the notch acuity:

$$\delta\left(\frac{a}{\rho}, 2\alpha\right) = 4.764\left(\frac{a}{\rho}\right)^{-0.180} + 1.479\,(2\alpha)^{2.000} - 2.002(2\alpha) \quad \text{for} \quad 4 \le a/\rho \le 25 \quad \text{and} \quad 0 \le 2\alpha \le 3\pi/4 \tag{7}$$

$$\delta\left(\frac{a}{\rho}, 2\alpha\right) = 4.764\left(\frac{a}{\rho}\right)^{-0.180} + 1.232\,(2\alpha)^{2.000} - 1.150(2\alpha) \quad \text{for} \quad 60 \le a/\rho \le 400 \quad \text{and} \quad 0 \le 2\alpha \le 3\pi/4 \tag{8}$$

When $25 < a/\rho < 60$, Eq. 7 or 8 can be used alternatively.

5 Evaluation of the J-integral under linear elastic conditions

The expression of the J-integral, considering only the notch arc contribution of a blunt V-notch (and excluding the contribution of the rectilinear flanks) can be written in the case of a generic opening angle (different from zero) as follows:

$$J = \int_{-\pi/2+\alpha}^{\pi/2-\alpha} W(\theta)\rho\cos(\theta)d\theta. \tag{9}$$

Here, the value of $W(\theta)$ for mode I loading can be calculated by means of the equations reported in paragraphs 3 and 4. A synthesis of all formulas for the exponent δ is given also in Table 2 considering both linear and nonlinear elastic conditions. It should be noted that Eq. 9 can be applied not only to the entire arc but also to an incomplete arc, by simply reducing in a symmetric way the integration limits.

Under plane strain conditions, the stress state at the notch tip is obviously biaxial, and the maximum value of the strain energy density $W_{\max}$ can be linked to the Beltrami equivalent stress $\sigma^B_{\max}$:

$$\begin{aligned} W_{\max} &= \frac{1}{2E}(\sigma^B_{\max})^2 = \frac{1}{2E}\left(\sigma^2_{y,apex} + \sigma^2_{z,apex}\right. \\ &\quad \left. -2\nu\left(\sigma_{y,apex}\sigma_{z,apex}\right)\right) \\ &= \frac{1}{2E}\sigma^2_{y,apex}\left(1-\nu^2\right), \end{aligned} \tag{10}$$

where y is the direction normal to the notch bisector, in the plate plane, z is the direction normal to the plate surface and ν is Poisson's ratio. Taking into account Eqs. 3 and 10, Eq. 9 can be rewritten as follows:

$$\begin{aligned} J_e &= \frac{\rho\left(\sigma^B_{\max}\right)^2}{E}\int_0^{\pi/2-\alpha}(\cos(\theta))^{\delta+1}d\theta \\ &= \frac{\rho\left(1-\nu^2\right)\left(\sigma_{y,apex}\right)^2}{E}\int_0^{\pi/2-\alpha}(\cos(\theta))^{\delta+1}\,d\theta. \end{aligned} \tag{11}$$

This equation is not fully analytical because the evaluation of the value of J_e depends on the stress $\sigma_{y,apex}$ at the notch tip. If the theoretical stress concentration factor $K_{t,g}$ referred to the gross area of the specimen is known, Eq. 11 becomes:

Table 2 Summary of the equations for the exponent δ in the case of mode I loading

	Linear elastic behaviour (plane strain conditions)	Nonlinear elastic behaviour (plane strain conditions)
U-notches	Lateral $\delta = 3.005\left(\frac{a}{\rho}\right)^{-0.112}$ for $4 \le a/\rho \le 400$ Central $\delta = 4.764\left(\frac{a}{\rho}\right)^{-0.180}$ for $4 \le a/\rho \le 400$	Lateral $\delta = 3.585\left(\frac{a}{\rho}\right)^{-0.209}$ for $4 \le a/\rho \le 400$ Central $\delta = 5.415\left(\frac{a}{\rho}\right)^{-0.232}$ for $4 \le a/\rho \le 400$
V-notches	Lateral $\delta = 3.005\left(\frac{a}{\rho}\right)^{-0.112} + 0.335\,(2\alpha)^{3.10}$ for $\begin{cases} 4 \le a/\rho \le 400 \\ 0 \le 2\alpha \le 3\pi/4 \end{cases}$ Central $\delta = 4.764\left(\frac{a}{\rho}\right)^{-0.180} + 1.479\,(2\alpha)^{2.000} - 2.002(2\alpha)$ for $\begin{cases} 4 \le a/\rho \le 25 \\ 0 \le 2\alpha \le 3\pi/4 \end{cases}$ $\delta = 4.764\left(\frac{a}{\rho}\right)^{-0.180} + 1.232\,(2\alpha)^{2.000} - 1.150(2\alpha)$ for $\begin{cases} 60 \le a/\rho \le 400 \\ 0 \le 2\alpha \le 3\pi/4 \end{cases}$	Lateral $\delta = 3.858\left(\frac{a}{\rho}\right)^{-0.209} + 0.082(2\alpha)^{4.75}$ for $\begin{cases} 4 \le a/\rho \le 400 \\ 0 \le 2\alpha \le 3\pi/4 \end{cases}$ Central $\delta = 5.415\left(\frac{a}{\rho}\right)^{-0.232} + 0.496(2\alpha)^{3.20} - 1.186\,(2\alpha)^{1.60}$ for $\begin{cases} 4 \le a/\rho \le 25 \\ 0 \le 2\alpha \le 3\pi/4 \end{cases}$ $\delta = 5.415\left(\frac{a}{\rho}\right)^{-0.232} + 0.494(2\alpha)^{3.20} - 0.771\,(2\alpha)^{1.60}$ for $\begin{cases} 60 \le a/\rho \le 400 \\ 0 \le 2\alpha \le 3\pi/4 \end{cases}$

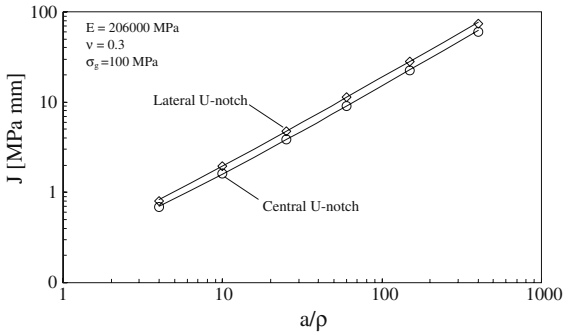

Fig. 7 Comparison between J evaluated using Eq. 12 and FE results for lateral and central U-notches under linear elastic conditions

$$J_e = \frac{\rho\left(1-\nu^2\right)\left(K_{t,g}\sigma_g\right)^2}{E}\int_0^{\pi/2-\alpha}(\cos(\theta))^{\delta+1}d\theta. \tag{12}$$

The results of the J-integral predicted on the basis of Eq. 12 are consistent with those obtained by processing results from FE analysis. Figure 7 shows a very good agreement between Eq. 12 and numerical results for central and lateral U-shaped notches. The same comparison is made in Table 3 for V-notches. Here, the maximum difference is 3.8% for the lateral notches and 3.7% for the central notches.

6 Strain energy density for U-notches in the case of a nonlinear elastic material

The aim is to analyse the role played by the stress level and the hardening exponent n on the exponent δ in Eq. 3 for a material obeying a power hardening law during the loading phase, excluding unloading or cyclic loading conditions (Anderson 2005).

A number of FE calculations have been carried out considering two steels and varying the notch acuity, as well as the applied stress σ_g in the gross sectional area (normalized with respect to the yield stress of the material). The trend of the strain energy density along the arc of a lateral U-notch tip is shown in Fig. 8 for different stress levels and different values of the notch acuity. In order to clearly represent in the same figure the trend of the strain energy density at different load levels, a multiplying factor η has been used. The factor η is reported in the caption of Fig. 8.

It can be seen that the exponent δ depends only on the notch acuity a/ρ, i.e. the value of δ is the same at the same acuity for the two different materials with very different hardening exponents n. Figure 8 shows also that the exponent δ tends to unity as the ratio a/ρ increases. For high values of the a/ρ ratio, the equation proposed by Matvienko and Morozov (2004) for U-notches is fully justified.

The exponent δ is a function of the notch acuity for central notches, as in the case of lateral notches, but its values are higher than in the previous case. For the two steels under consideration, Fig. 9 plots the strain energy density along the notch arc for different stress levels ($\bar{\sigma} = \sigma_g/\sigma_0 = 0.2;\ 0.4;\ 0.6;\ 0.8$). In parallel, the ratio a/ρ ranges from 4 to 400. Also, in this case a multiplied factor η has been used to avoid the curves overlapping.

The values of the exponent δ are found to be close to the values obtained under linear elastic conditions when the notch acuity a/ρ is less than or equal to 25 in the case of central notches, less than or equal to 10 in the case of lateral notches (see again Table 1). The differences, probably due also to numerical errors, should mainly depend on the different values of Poisson's ratio ν characterising the notch tip under linear elastic ($\nu = 0.3$) and nonlinear elastic conditions ($\nu = 0.5$). For deep notches, a plastic zone is present also under low stress levels and the differences due to different values of ν are higher than for notches having low notch acuity. Moreover, there is a transition zone ahead of the notch where the value of ν gradually tends to approach the value of 0.3 characterising the zones far from the notch tip.

By using the values of δ listed in Table 1 for lateral and central U-notches under mode I loading for a power hardening material, the following equations have been obtained. For lateral U-notches we have:

$$\delta = 3.585\left(\frac{a}{\rho}\right)^{-0.209} \quad \text{for} \quad 4 \le a/\rho \le 400 \tag{13}$$

For central U-notches the equation is:

$$\delta = 5.415\left(\frac{a}{\rho}\right)^{-0.232} \quad \text{for} \quad 4 \le a/\rho \le 400 \tag{14}$$

Table 3 Comparison between J evaluated using Eq. 12 and J from FE results (for a nominal stress $\sigma_g = 100\,\text{MPa}$); lateral and central V-notches under linear elastic conditions

		Lateral V-notches				Central V-notches			
2α [rad]	a/ρ	$\sigma^{\text{B}}_{\text{max}}$ [MPa]	J_{FEM} [MPamm]	J [MPamm]	Δ [%] $\frac{\text{J}_{\text{FEM}}-\text{J}}{\text{J}_{\text{FEM}}} \times 100$	$\sigma^{\text{B}}_{\text{max}}$ [MPa]	J_{FEM} [MPamm]	J [MPamm]	Δ [%] $\frac{\text{J}_{\text{FEM}}-\text{J}}{\text{J}_{\text{FEM}}} \times 100$
$\pi/3$	4	535.1	0.78	0.80	−3.37	531.7	0.77	0.78	−1.14
	10	803.5	1.83	1.88	−2.66	785.3	1.80	1.80	−0.32
	25	1230.1	4.40	4.52	−2.70	1191.2	4.28	4.37	−2.12
	60	1866.3	10.24	10.62	−3.79	1798.8	9.93	9.71	2.20
	150	2902.7	25.90	26.25	−1.36	2791.0	24.12	24.33	−0.88
	400	4671.9	67.67	69.46	−2.64	4466.5	62.57	64.71	−3.42
$\pi/2$	4	529.4	0.69	0.69	−0.15	542.0	0.72	0.71	0.60
	10	783.4	1.55	1.54	0.15	795.3	1.59	1.59	−0.49
	25	1175.2	3.51	3.53	−0.63	1188.6	3.58	3.69	−2.87
	60	1742.2	7.73	7.87	−1.76	1759.3	7.88	7.88	0.06
	150	2638.4	17.76	18.30	−3.05	2662.3	18.08	18.50	−2.35
	400	4118.5	43.83	45.20	−3.11	4136.9	44.10	45.74	−3.72
$3\pi/4$	4	424.3	0.28	0.28	−0.63	459.0	0.33	0.33	−0.95
	10	569.8	0.50	0.51	−1.09	615.2	0.59	0.60	−2.10
	25	767.2	0.91	0.93	−1.57	827.6	1.06	1.10	−3.17
	60	1020.2	1.62	1.65	−2.00	1100.4	1.88	1.93	−2.60
	150	1375.5	2.94	3.01	−2.42	1483.2	3.42	3.53	−3.40
	400	1894.3	5.57	5.73	−2.83	2022.7	6.48	6.62	−2.10

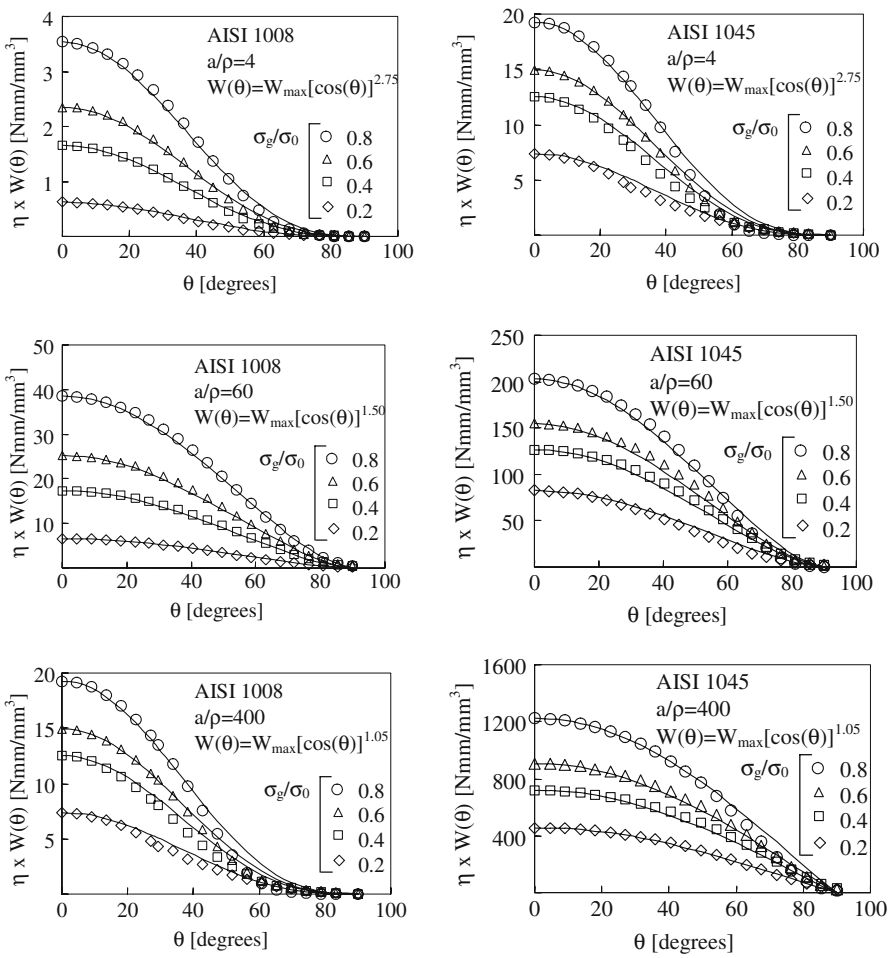

Fig. 8 Strain energy density along the notch edge for lateral U-notches having different acuity a/ρ. Different stress levels have been applied ($\sigma = \sigma_g/\sigma_0 = 0.2, 0.4, 0.6, 0.8$). For the AISI 1008 the multiplying factor η was equal to 10, 5, 2, 1 for the ratio $\sigma_g/\sigma_0 = 0.2, 0.4, 0.6, 0.8$, respectively. For the AISI 1045 $\eta = 10, 5, 4, 1$ for the ratio $\sigma_g/\sigma_0 = 0.2, 0.4, 0.6, 0.8$, respectively

7 Strain energy density for V-notches in the case of a nonlinear elastic material

The strain energy density was evaluated considering also lateral and central V-notches under mode I loading. As in the case of U-notches, firstly lateral notches have been considered. Several FE calculations have been carried out to analyze the influence played on the exponent δ by the stress level, the hardening exponent, the notch acuity and the opening angle. As an example, Fig. 10 shows the trend of the strain energy density $W(\theta)$ along the semicircular arc of a V-notch for a normalised stress ratio equal to 0.6. Also in this case a multiplying factor η is used to show clearly the three curves corresponding to the different opening angles, avoiding their overlapping. Here, the plate is made of AISI 1045. The exponent δ does depend on the notch angle and the notch acuity, not on the stress level and the hardening exponent n.

With reference to lateral V-notches, the equation for δ is:

$$\delta\left(\frac{a}{\rho}, 2\alpha\right) = 3.858\left(\frac{a}{\rho}\right)^{-0.209} + 0.082(2\alpha)^{4.75} \quad \text{for} \quad 60 \le a/\rho \le 400 \quad \text{and} \quad 0 \le 2\alpha \le 3\pi/4 \tag{15}$$

For central V-notches, δ varies according to the following laws:

$$\delta\left(\frac{a}{\rho}, 2\alpha\right) = 5.415\left(\frac{a}{\rho}\right)^{-0.232} + 0.496(2\alpha)^{3.20} - 1.186\,(2\alpha)^{1.60} \quad \text{for} \quad 4 \le a/\rho \le 25 \quad \text{and} \quad 0 \le 2\alpha \le 3\pi/4 \tag{16}$$

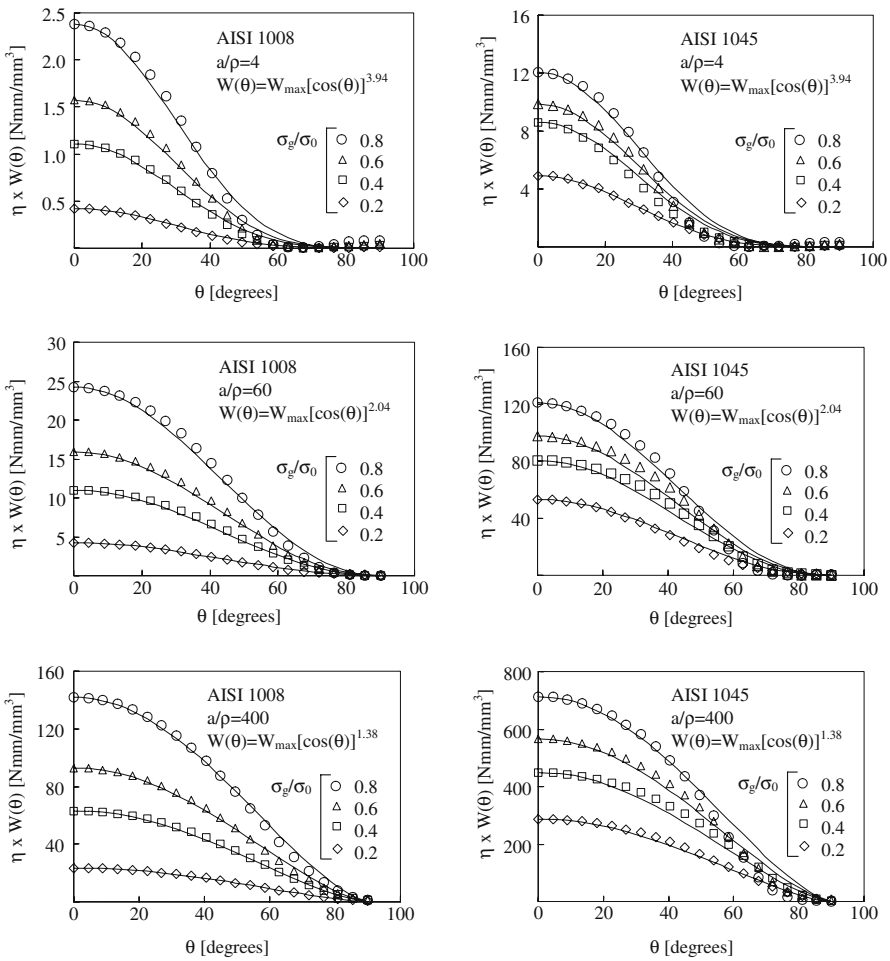

Fig. 9 Strain energy density along the notch edge for central U-notches having different acuity a/ρ. Different stress levels have been applied ($\sigma = \sigma_g/\sigma_0 = 0.2, 0.4, 0.6, 0.8$). For the AISI 1008 the multiplying factor η was equal to 10, 5, 2, 1 for the ratio $\sigma_g/\sigma_0 = 0.2, 0.4, 0.6, 0.8$, respectively. For the AISI 1045 $\eta = 10, 5, 4, 1$ for the stress ratio $\sigma_g/\sigma_0 = 0.2, 0.4, 0.6, 0.8$, respectively

$$\delta\left(\frac{a}{\rho}, 2\alpha\right) = 5.415\left(\frac{a}{\rho}\right)^{-0.232} + 0.494(2\alpha)^{3.20} - 0.771\,(2\alpha)^{1.60} \quad \text{for} \quad 60 \le a/\rho \le 450 \quad \text{and} \quad 0 \le 2\alpha \le 3\pi/4 \tag{17}$$

8 Evaluation of the J-integral in the case of a nonlinear elastic material

Equations 9 and 3 have been employed in combinations to estimate the J-integral for U- and V-blunt notches in a power hardening material under mode I loading. (For a complete synthesis, see also Table 2).

For materials that follow the Ramberg-Osgood law, the maximum value of the strain energy density $W_{\max}$ can be evaluated by means of the following equation:

$$W_{\max} = \frac{1}{2E}\left(\sigma^{\mathrm{B}}_{\max}\right)^2 + \frac{n}{n+1}\left(\frac{\left(\sigma^{\mathrm{B}}_{\max}\right)^{n+1}}{K^n}\right) \tag{18}$$

Under plane strain conditions, the Beltrami stress at the notch tip turns out to be

$$\sigma^{\mathrm{B}}_{\max} = \sqrt{\sigma^2_{\mathrm{y,apex}} + \sigma^2_{\mathrm{z,apex}} - 2\nu\sigma_{\mathrm{y,apex}}\sigma_{\mathrm{z,apex}}} = \sqrt{\sigma^2_{\mathrm{y,apex}} + \left(\nu\sigma_{\mathrm{y,apex}}\right)^2 - 2\nu\sigma_{\mathrm{y,apex}}\left(\nu\sigma_{\mathrm{y,apex}}\right)} \tag{19a}$$

$$\sigma^{\mathrm{B}}_{\max} = \sigma_{\mathrm{y,apex}}\sqrt{1-\nu^2}, \tag{19b}$$

where $\sigma_{\mathrm{y,apex}}$ and $\sigma_{\mathrm{z,apex}}$ are the two principal stresses, both different from zero, at the notch tip.

Note that, differently from the maximum principal stress that is not located at the notch tip, the Beltrami stress reaches its maximum value at the notch tip. It

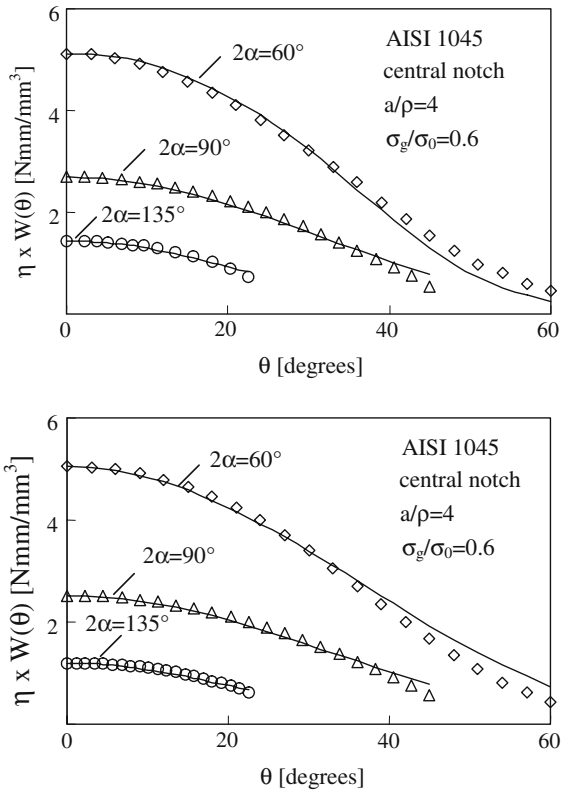

Fig. 10 Strain energy density along the notch edge for blunt central and lateral V-notches for $a/\rho = 4$. The multiplying factor, η, was equal to1/2 and 1/3 for $2\alpha = 90°$ and 135°, respectively

is also worth noting that for a nonlinear behaviour of the material the Beltrami equivalent stress coincides with the von Mises equivalent stress when ν is equal to 0.5. Obviously, the equivalent stress allows us to quantify the stress state at the notch tip and it is due to the presence of two principal stresses different from zero, being also σ_z different from zero under plane strain conditions.

By including Eq. 18 into Eq. 9, the J-integral can be given as a function of the Beltrami stress:

$$J = 2\rho \left[\frac{\left(\sigma^{B}_{max}\right)^2}{2E} + \frac{n}{n+1} \frac{\left(\sigma^{B}_{max}\right)^{n+1}}{K^n} \right] \times \int_0^{\pi/2-\alpha} (\cos(\theta))^{\delta+1} d\theta \quad (20)$$

Again, it should be noted that Eq. 20 is not fully analytical because the Beltrami stress at the notch apex should be evaluated with the FE method or with approximate equations (Neuber's rule; the Equivalent Strain Energy Density criterion; Molski and Glinka 1981; Glinka 1985).

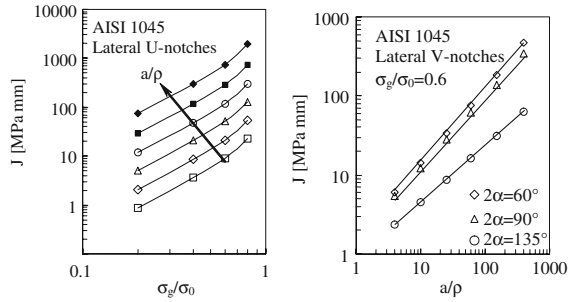

Fig. 11 Comparison between J evaluated using Eq. 20 and FE results for lateral U- and V-notches in the case of a power hardening material (AISI 1045). Different values of the notch acuity for blunt U-notches have been considered ($a/\rho = 4$, 10, 25, 60, 150, 400)

Some comparisons have been carried out between Eq. 20 and FE results both for U- and V-notches (Fig. 11). A more complete synthesis is given in Table 4 (AISI 1008 and AISI 1045, lateral and central U-notches, $\sigma_g/\sigma_0 = 0.8$), Table 5 (AISI 1008, lateral and central V-notches, with σ_g/σ_0 equal to 0.8 or 0.6, respectively) and Table 6 (AISI 1045, lateral and central V-notches, with σ_g/σ_0 equal to 0.6).The agreement between the FE results and the analytical ones is good enough for all considered cases. The maximum difference is found to be 2.5% for U-notches (Table 4), 5.8% for V-notches made of AISI 1008 (Table 5) and 5.3% for V-notches made of AISI 1045 (Table 6).

9 Some links between the J-integral and the strain energy

Equation 3 for W cannot be applied to sharp, zero radius, V-notches (*i.e.* for re-entrant corners), nor permits to account for the contribution to J provided by the straight flanks in the case of blunt V-notches.

These limitations are overcome in Fig. 12 where all results are determined by means of FE analyses. In particular, a plate made of AISI 1008 with two symmetric notches is considered, like that already shown in Fig. 2a. The notch depth a and the notch opening angle 2α are 14 mm and 135°, respectively, whereas the ligament width, $B - 2a$, is 28 mm. Two values are considered for the notch root radius, 0 and 1 mm. Finally, the material is modelled according to a linear elastic law or a power strain hardening law.

Table 4 Comparison between J evaluated using Eq. 20 and J from FE results; lateral and central U-notches for a power hardening material

	a/ρ	σ_g/σ_0	σ^B_{max} [MPa]	J_{FEM}[MPamm]	J [MPamm]	$\Delta\% \frac{J_{FEM}-J}{J_{FEM}} \times 100$	σ^B_{max} [MPa]	J_{FEM}[MPamm]	J [MPamm]	$\Delta\% \frac{J_{FEM}-J}{J_{FEM}} \times 100$
AISI 1008			U-Lateral				U-Central			
	4	0.8	224.2	4.38	4.39	−0.11	206.7	2.61	2.61	0.14
	10	0.8	262.1	10.24	10.12	1.19	240.9	5.99	5.96	0.63
	25	0.8	309.3	24.53	24.28	1.04	283.0	14.26	14.13	0.93
	60	0.8	364.8	57.35	57.79	−0.76	332.2	33.23	33.23	0.02
	150	0.8	432.3	140.72	140.44	0.20	395.1	81.41	83.43	−2.48
	400	0.8	521.7	369.95	372.07	−0.57	473.3	213.93	216.95	−1.41
AISI 1045			U-Lateral				U-Central			
	4	0.8	628.4	23.00	22.86	0.62	597.2	12.67	12.90	−1.83
	10	0.8	684.3	53.75	52.98	1.42	649.5	29.07	29.38	−1.08
	25	0.8	748.9	128.44	128.23	0.16	708.1	69.20	69.17	0.04
	60	0.8	815.0	299.08	294.07	1.67	771.4	161.34	161.66	−0.20
	150	0.8	894.6	733.50	729.15	0.59	844.9	397.02	398.56	−0.39
	400	0.8	986.9	1929.71	1887.92	2.17	932.5	1045.58	1054.42	−0.84

Table 5 Comparison between J evaluated using Eq. 20 and J from FE results; lateral and central V-notches for a power hardening material (AISI 1008)

2α [rad]	a/ρ	σ_g/σ_0	σ^{B}_{max} [MPa]	J_{FEM} [MPamm]	J [MPamm]	$\Delta\% \frac{J_{FEM}-J}{J_{FEM}} \times 100$	σ_g/σ_0	σ^{B}_{max} [MPa]	J_{FEM} [MPamm]	J [MPamm]	$\Delta\% \frac{J_{FEM}-J}{J_{FEM}} \times 100$
		V-lateral					V-central				
$\pi/3$	4	0.8	200.4	2.53	2.44	3.59	0.6	165.1	0.96	0.94	2.40
	10	0.8	235.2	5.88	5.62	4.35	0.6	193.2	2.22	2.16	2.87
	25	0.8	277.1	13.87	13.22	4.71	0.6	227.8	5.22	5.17	0.97
	60	0.8	326.2	31.79	30.89	2.83	0.6	267.9	11.91	11.52	3.35
	150	0.8	388.4	76.25	76.37	−0.16	0.6	319.1	28.45	28.81	−1.26
	400	0.8	467.4	195.33	198.77	−1.77	0.6	383.3	72.63	75.16	−3.48
$\pi/2$	4	0.8	199.3	2.26	2.12	5.81	0.6	167.7	0.95	0.93	2.41
	10	0.8	233.1	4.96	4.74	4.52	0.6	195.4	2.07	2.04	1.51
	25	0.8	274.4	11.11	10.92	1.65	0.6	229.4	4.61	4.68	−1.49
	60	0.8	321.3	24.22	24.50	−1.14	0.6	268.3	10.01	9.83	1.78
	150	0.8	378.6	55.11	56.73	−2.94	0.6	316.9	22.71	23.14	−1.92
	400	0.8	450.0	133.31	137.01	−2.78	0.6	377.1	54.81	56.58	−3.23
$3\pi/4$	4	0.8	182.3	0.88	0.85	3.86	0.6	155.7	0.42	0.40	3.49
	10	0.8	206.7	1.62	1.57	2.84	0.6	176.8	0.76	0.75	1.57
	25	0.8	234.4	2.99	2.93	1.90	0.6	200.8	1.41	1.41	−0.27
	60	0.8	264.4	5.39	5.35	0.85	0.6	226.9	2.54	2.50	1.46
	150	0.8	300.0	10.02	10.06	−0.41	0.6	257.5	4.71	4.69	0.13
	400	0.8	343.3	19.46	19.74	−1.43	0.6	294.4	9.13	9.19	−0.63

Table 6 Comparison between J evaluated using Eq. 20 and J from FE results; lateral and central V-notches for a power hardening material (AISI 1045)

2α [rad]	a/ρ	σ_g/σ_0	$\sigma^B_{\max}$ [MPa]	J_{FEM} [MPamm]	J [MPamm]	$\Delta\% \frac{J_{FEM}-J}{J_{FEM}} \times 100$	$\sigma^B_{\max}$ [MPa]	J_{FEM} [MPamm]	J [MPamm]	$\Delta\% \frac{J_{FEM}-J}{J_{FEM}} \times 100$
		V-lateral					V-central			
$\pi/3$	4	0.6	539.3	6.01	5.84	2.83	537.8	5.79	5.57	3.78
	10	0.6	591.9	14.17	13.64	3.76	588.1	13.57	12.92	4.80
	25	0.6	647.8	33.65	31.99	4.94	645.2	32.13	31.61	1.61
	60	0.6	706.0	76.58	72.89	4.82	703.7	73.24	69.82	4.67
	150	0.6	775.2	182.62	178.75	2.12	769.5	174.39	167.59	3.90
	400	0.6	856.7	466.30	467.43	−0.24	853.3	444.10	457.86	−3.10
$\pi/2$	4	0.6	538.4	5.44	5.15	5.32	542.8	5.73	5.51	3.73
	10	0.6	589.6	12.27	11.60	5.44	592.8	12.84	12.41	3.33
	25	0.6	645.3	27.79	26.77	3.64	648.6	28.95	29.02	−0.23
	60	0.6	702.1	60.95	59.20	2.86	705.6	63.28	60.72	4.05
	150	0.6	767.1	139.65	136.96	1.92	770.2	144.91	140.39	3.12
	400	0.6	847.0	342.51	350.33	−2.28	850.7	354.43	363.16	−2.461
$3\pi/4$	4	0.6	516.6	2.38	2.25	5.35	527.6	2.85	2.71	4.62
	10	0.6	558.4	4.50	4.33	3.93	568.5	5.37	5.16	3.87
	25	0.6	601.9	8.60	8.37	2.60	612.5	10.27	10.05	2.20
	60	0.6	646.1	16.07	15.90	1.08	657.1	19.18	18.42	3.96
	150	0.6	695.4	31.12	31.22	−0.31	706.7	37.11	36.06	2.83
	400	0.6	750.2	63.07	63.08	−0.02	763.0	75.34	73.68	2.20

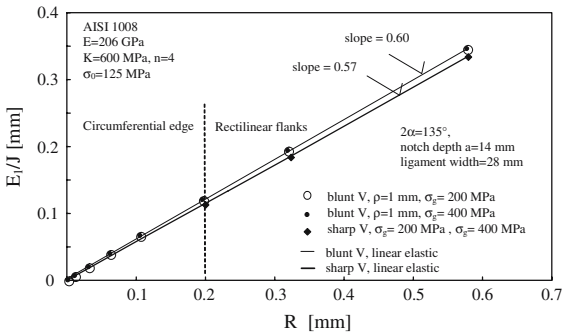

Fig. 12 E_1/J trend for sharp and blunt symmetric V-notches under nonlinear elastic conditions, as obtained from FE analyses; comparison with linear elastic FE results (nominal stress values σ_g related to the gross sectional area). Plots taken from (Berto and Lazzarin 2007)

Figure 12 plots E_1/J as a function of R_c, being E_1 the total strain energy evaluated on the control volume under plane strain conditions. The results from blunt V-notches under linear elastic conditions match those from notches under nonlinear elastic conditions, the latter obtained by applying two different values of the nominal stress, both greater than the yielding stress of the material to assure a large amount of plasticity. Also the results from sharp notches are coincident and very close to the previous ones. No discontinuity is present in the diagram for values of R_c greater or lower than 0.2 mm, which is the maximum value that assures a control volume embracing only the semicircular root.

10 Conclusions

Some approximate formulas to calculate the J-integral in plates with lateral and central U- and V-blunt notches under mode I loading have been obtained taking into account both a linear elastic and nonlinear elastic material, the latter being modelled according a power hardening law. It should be noted that suggested formulas are valid also for an elastic–plastic material if the material is not unloaded or cyclically loaded.

For the J-integral calculations the integration path has been assumed to be coincident with the semi-circular arc of the notch, which is traction free. Then, the contribution to the J-integral provided by the notch arc, and not that of the notch rectilinear flanks, has been evaluated in the case of V-notches.

The distribution of the strain energy density $W(\theta)$ on the surface of the notch arc has been assumed in the form $W(\theta) = W_{\max} \cos^{\delta}(\theta)$ as a result of an empirical guess based on matching numerical results for mode I loading.

A numerical investigation of the strain energy density, the exponent δ and the J-integral has been carried out considering a large variability of the notch acuity ($4 \leq a/\rho \leq 400$) and the opening angle ($0 \leq 2\alpha \leq 3/4\pi$). For materials obeying the Ramberg-Osgood law the results from the FE analysis have demonstrated that the exponent δ depends on the notch opening angle and the notch acuity a/ρ. It does not depend on the stress level and the hardening exponent n. The basic equations for the exponent δ have been summarized in a tabular form.

In order to calculate the strain energy density and then the J-integral for a body with notches, the equivalent stress at the notch tip should be known or calculated by means of the FEM or approximate equations. By using the approximate formulas suggested in the present paper for U- and V-blunt notches under mode I loading, the J-integral values for a linear and nonlinear elastic material are consistent with those directly obtained from FE analyses, the maximum errors being about equal to 5 percent.

Acknowledgements Professor Yu.G. Matvienko would like to thank the University of Padova for funding a visit to the Department of Management and Engineering, University of Padova. Furthermore, the authors appreciate the kind help from the Reviewers, who provided beneficial suggestions for improving the final version of the manuscript.

References

Anderson TL (2005) Fracture mechanics fundamentals and application. Taylor and Francis, New York

Atluri SN (ed) (1986) Computational methods in the Mechanics of Fracture. North Holland Pubbl. Co., Amsterdam

Berto F, Lazzarin P (2007) Relationships between J-integral and the strain energy evaluated in a finite volume surrounding the tip of sharp and blunt V-notches. Int J Solids Struct 44:4621–4645

Carpinteri A (1987) Stress singularity and generalised fracture toughness at the vertex of re-entrant corners. Eng Fract Mech 26:143–155

Cherepanov GP (1979) Mechanics of brittle fracture. McGraw-Hill, New York

Chen YH, Lu TJ (2004) On the path dependence of the J-integral in notch problems. Int J Solids Struct 41:607–618

Dowling NE (1993) Mechanical behaviour for deformation, facture and fatigue. Prentice-Hall International Edition

Dunn ML, Suwito W, Cunningham SJ (1997a) Fracture initiation at sharp notches: correlation using critical stress intensities. Int J Solids Struct 34:3873–3883

Dunn ML, Suwito W, Cunningham SJ, May CW (1997b) Fracture initiation at sharp notches under mode I, mode II, and mild mixed mode loading. Int J Fract 84:367–381

Gdoutos EE, Rodopoulos CA, Jates JR (2003) Problems of fracture mechanics and fatigue. Kluwer Academic Publishers, Dodrecht

Glinka G (1985) Energy density approach to calculation of inelastic strain-stress near notches and cracks. Eng Fract Mech 22:485–508

Gómez FJ, Elices M (2003) A fracture criterion for sharp V-notched samples. Int J Fract 123:163–175

Gómez FJ, Elices M (2004) A fracture criterion for blunted V-notched samples. Int J Fract 127:239–264

Gómez FJ, Elices M, Planas J (2005) The cohesive crack concept: application to PMMA at $-60°$C. Eng Fract Mech 72:1268–1285

Gómez FJ, Elices M, Berto F, Lazzarin P (2007) Local strain energy to assess the static failure of U-notches in plated under mixed mode loading. Int J Fract 145:29–45

Gross R, Mendelson A (1972) Plane elastostatic analysis of V-notched plates. Int J Fract Mech 8:267–276

Kumar V, German MD, Shih CF (1981) An engineering approach for elastic–plastic fracture analysis. EPRI report NP-1931, Electric Power Research Institute, Palo Alto

Kumar V, German MD, Wilkening WW, Andrew WR, deLorenzi HG, Mowbray DF (1984) Advances in elastic–plastic fracture analysis. EPRI Report NP-3607, Electric Power Research Institute, Palo Alto

Kumar V, German MD (1988) Elastic–plastic fracture analysis of through-wall and surface flaws in cylinders. EPRI report NP-5596, Electric Power Research Institute, Palo Alto

Lazzarin P, Zambardi R (2001) A finite-volume-energy based approach to predict the static and fatigue behaviour of components with sharp V-shaped notches. Int J Fract 112:275–298

Lazzarin P, Livieri P, Zambardi R (2002) 1A J-integral-based approach to predict the fatigue strength of components weakened by sharp V-shaped notches. Int J Comp Appl Technol 15(4/5):202–210

Lazzarin P, Lassen T, Livieri P (2003) A notch stress intensity approach applied to fatigue life predictions of welded joints with different local toe geometry. Fatigue Fract Eng Mater Struct 26:49–58

Lazzarin P, Berto F (2005a) Some expressions for the strain energy in a finite volume surrounding the root of blunt V-notches. Int J Fract 135:161–185

Lazzarin P, Berto F (2005b) From Neuber's elementary volume to Kitagawa and Atzori's diagrams: an interpretation based on local energy. Int J Fract 135:L33–L38

Livieri P (2003) A new path independent integral applied to notched components under mode I loadings. Int J Fract 123:107–125

Livieri P, Lazzarin P (2005) Fatigue strength of steel and aluminium welded joints based on generalised stress intensity factors and local strain energy values. Int J Fract 133:247–276

Matvienko YuG (1994) J-estimation formulas for non-linear crack problems. Int J Fract 68:R15–R18

Matvienko YuG, Morozov EM (2004) Calculation of the energy J-integral for bodies with notches and cracks. Int J Fract 125:249–261

Molski K, Glinka G (1981) A method of elastic–plastic stress and strain calculation at a notch root. Mater Sci Eng 50:93–100

Neuber H (1958) Kerbspannungslehre, 2nd edn. Springer-Verlag, Berlin

Neuber H (1985) Kerbspannungslehre, 3rd edn. Springer-Verlag, Berlin

Pluvinage G (2003) Fracture and fatigue emanating from stress concentrators. Kluwer Academic Publishers, Dodrecht

Rice JR (1968) A path independent integral and the approximate analysis of strain concentration by notches and cracks. J Appl Mech 35:379–386

Saxena A (1998) Nonlinear fracture mechanics for engineering. CRC press, Boca Raton

Seweryn A (1994) Brittle fracture criterion for structures with sharp notches. Eng Fract Mech 47:673–681

Seweryn A, Poskrobko S, Mróz Z (1997) Brittle fracture in plane elements with sharp notches under mixed-mode loading. J Eng Mech 123:535–543

Shih CF, Hutchinson JW (1976) Fully plastic solutions and large-scale yielding estimates for plane stress crack problems. J Eng Mater Technol 98:289–295

Williams ML (1952) Stress singularities resulting from various boundary conditions in angular corners of plates in extension. J Appl Mech 19:526–528

Yosibash Z, Bussiba AR, Gilad I (2004) Failure criteria for brittle elastic materials. Int J Fract 125:307–333

Zahoor A (1989) Ductile fracture handbook, vol 1. Circumferential Through cracks. EPRI report NP. 6301 D, Electric Power Research Institute, Palo Alto